1973

Threshold crack growth in A36 steel, September 1973

David J. Klingerman

John W. Fisher

OFFICE
OF
RESEARCH

LEHIGH UNIVERSITY

High Cycle Fatigue of
Welded Bridge Details

THRESHOLD CRACK GROWTH IN A36 STEEL

by
David J. Klingerman
John W. Fisher

Fritz Engineering Laboratory Report No. 386.2

ACKNOWLEDGMENTS

This investigation was part of PennDOT Research Project 72-3, a study of high cycle fatigue of welded bridge details sponsored by the Pennsylvania Department of Transportation and the Federal Highway Administration. The testing program was accomplished at Fritz Engineering Laboratory, Department of Civil Engineering, Lehigh University. Dr. Lynn S. Beedle is the director of Fritz Laboratory, and Dr. David A. VanHorn is the head of the Civil Engineering Department.

The specimens were fabricated in the machine shops of Fritz Engineering Laboratory and Whitaker Laboratory. Mr. Richard N. Sopko prepared the photographs. Figures and graphs were drawn by Mr. John M. Gera and Mr. David E. VanCott. Typing of the manuscript was performed by the word processing center.

Thanks are also due Drs. B. T. Yen and R. G. Slutter for their assistance and suggestions during the conduct of this study.

TABLE OF CONTENTS

		Page
1.	INTRODUCTION	1
2.	DESCRIPTION OF TEST SPECIMENS	4
3.	TESTING APPARATUS AND TECHNIQUES	6
4.	TEST RESULTS	9
	4.1 Strain Gage Results for Gripping Effect	9
	4.2 Observed Loading Effects	11
	4.3 Graphic Results	13
5.	ANALYSIS OF DATA	13
	5.1 Fracture Mechanics Analysis	15
	5.2 Comparison with Complementary Crack Growth Investigation	15
	5.3 Threshold and High Cycle Fatigue	16
	5.4 Effect of Minimum Stress	17
	5.5 Correlation with Coverplated Beam Studies	18
6.	CONCLUSIONS	24
	NOMENCLATURE	27
	TABLES	29
	FIGURES	36
	REFERENCES	53

LIST OF TABLES

Table		Page
1	Material Properties of 3/8" A36 Rolled Plate	29
2	Material Properties of Rolled A36 Flange	29
3	Crack Growth Data for Center-Notched Specimens from A36 Steel Plate	30
4	Crack Growth Data for Center-Notched Specimens from A36 Steel Beam Flange	34
5	Threshold Values of Stress Intensity Range	36

LIST OF FIGURES

Figure		Page
1	Origin of Specimens	36
2	Geometry of Specimen and Center Notch	37
3	Specimen Mounted in Testing Machine	38
4	Close-Up of Specimen in Grips	39
5	Cracks Emanating from Center Notch	40
6	Notch Tip and Crack Viewed through Microscope	41
7	Crack Length Defined on Fracture Surface	42
8	Strain Gages Mounted on Specimen	43
9	Typical Exposed Fracture Surface	44
10	Comparison of Load History and Observed Banding	45
11	Typical a vs. N Plot Comparing Average, Left and Right Crack Sizes	46
12	Crack Propagation Data and Mean Line for Welded Beams	47
13	Summary of Fatigue Crack Growth for A36 Steel	48
14	Critical Regions of Fatigue Crack Propagation	49
15	Effect of the Minimum Stress Variable	50
16	Geometry of Cover Plate Welded to Beam Flange	51
17	Cover-Plated Beam Failures and Predicted Runout	52

1. INTRODUCTION

The importance of fatigue in structural design has long been recognized, but an exact description of this phenomenon has proven difficult to achieve. For welded details, fatigue, or the process of initiation of microscopic cracks and their propagation to macroscopic size during repeated application of load has been shown to be dependent upon the range of applied stress and the geometry of a particular detail.[1][2] The current approach to fatigue design of bridges and buildings is to specify allowable magnitudes for the stress range in a given detail based on the proposed structural life or number of loading cycles to which the structure will be subjected while in operation.[3][4] This approach has proven to be satisfactory for designing most structures subjected to fatigue loading.

In the past no limitation for stress range has been specified for a bridge design life of more than two million cycles of load. Due to the extended use of such fatigue-critical structures as highway bridges and overhead cranes in mill buildings, many structures can be expected to be subjected to more than two million cycles before their planned replacement. Previous research on beams with welded details[1][5] has shown that fatigue cracking developed in structural details subjected to lower levels of stress range at well over two million cycles of loading. This observation points out the need for more extensive studies on high cycle - low stress fatigue.

The purpose of this study is to determine a threshold stress range parameter for which no crack propagation will occur under high cycle fatigue conditions. Most previous crack growth studies

have concentrated on high strength steel and high rates of growth. The majority of bridge structures in service today, however, have been constructed with mild strength steel such as A36 steel. Due to its previous and continuing popularity and the lack of knowledge about its fatigue crack propagation behavior at low stress levels, A36 steel was selected for this investigation.

Besides searching for a threshold of crack growth an attempt was made to simulate crack growth in welded details. The specific detail examined was the cover-plated beam since it has been found to be the most critical welded detail in fatigue.[5] Due to the existence of large residual stresses at the site of most welded details it was desired to introduce a similar situation into the crack growth specimens by statically applying high minimum loads which remained constant while cyclic load was applied. This technique produced residual stresses at the cracked net section which approached the yield strength of the material.

A total of eight crack growth specimens were tested to accumulate crack growth data at very low growth rates. These specimens were tested under laboratory conditions with no specially induced environments. In several specimens for certain levels of stress range no crack growth occurred. These situations are reported as runout conditions since it was judged highly unlikely that a fatigue crack problem would develope in a structural detail subjected to a similar number of cycles of loading. In cases were crack growth resulted, measurements were taken at frequent intervals to provide as much data from specimens as possible. This data along with the runout conditions was used

to predict a runout condition for the beams. Because of the differences in geometry an analytical method was necessary to make the correlation between the specimens and beams.

Since its inception fracture mechanics has proven to be a valuable tool in analyzing the stress conditions which exist at the tip of a propagating crack. By choosing a specimen geometry in which fracture mechanics enabled the stress conditions to be quite accurately defined, a good control was established. The stress conditions which would produce no crack growth in the tested specimens should likewise produce no propagation of cracks from discontinuities in the welded cover-plated beams. A mathematical model developed elsewhere[5][6] was used to determine the approximate stress conditions at the end of the coverplate. The ultimate purpose of this phase of the investigation was to predict a threshold stress range below which no crack growth would occur in beams with coverplates welded to the flanges.

2. DESCRIPTION OF TEST SPECIMENS

All specimens were made from ASTM A36 steel plate. The majority of specimens were fabricted from rolled steel plate, however, several were taken from the flange of one of the previously tested coverplated beams to determine if any difference existed for different sources of the material. Material properties as obtained by ASTM standard tensile tests are reported in Table 1 for the plate material and Table 2 for the flange material.

Specimens were cut as shown in Fig. 1 from the rolled 3/8 in. plate and the rolled W14 x 30 beam. Care was taken to maintain the longitudinal axis of the specimens along the direction of rolling. This was desired since the largest tensile stresses in a structural element usually occur parallel to the direction of rolling of that element. The end portions of both the plate and the beam were discarded to reduce the amount of residual stresses of unknown magnitude which might have been present in the specimens.

All specimens were machined to the configuration shown in Fig. 2. The length, L, was limited to 10 in. for some specimens by the capacity of the machine which was used to notch them. All other specimens notched on a larger machine were limited to a 12 in. length by the travel of the testing machine. A width, W, of 3.75 in. was selected for the specimens cut from the rolled plate to accomodate the capacity of the machine. In order to reduce the possibility of high residual stresses in the vicinity of the center notch the specimens were cut from the beam flange as shown in Fig. 1. This choice allowed a

maximum width of 3.25 in. leaving these specimens insignificantly narrower than the other specimens. Excess material from the flange specimens was removed from the width on the side containing the flange tip to insure a final uniformly-sized specimen and reduce the chance of residual stresses. A smooth uniform surface was achieved on each specimen by a milling and grinding process on both faces wich reduced the thickness to 0.250 ± 0.015 in. for all specimens as shown in Fig. 2.

After all specimens were machined to size, a 1/8 in. hole was drilled in the center of the specimen to facilitate placing of the starter notch. From each side of this hole and extending in a direction perpendicular to the longitudinal axis of the specimen a starter notch was machined into the specimen by the electrical discharge process. Details of this notch also appear in Fig. 2. The surface of the specimen in the vicinity of the notch was then polished with fine grades of emery paper to facilitate crack observation.

Several specimens were stress relieved at 1150° Fahrenheit then furnace cooled after all machining was accomplished to ascertain the degree to which machining introduced residual stresses. By measuring the amount of warp in the specimen before and after stress relief it was found that machining did not introduce any significant stresses into the specimen.

3. TESTING APPARATUS AND TECHNIQUES

In view of the fact that the growth rates would be extremely slow a machine was needed which could cycle the load at a very fast rate. The machine selected was the Amsler High Frequency Vibrophore, pictured in Fig. 3, which applied the load range at a rate of 11,500 CPM. A ten-metric-ton dynamometer was employed to allow a maximum load of 22.0 kips in tension which provided a tensile load range of 22.0 kips with an accuracy of $\pm$ 1.5% but less than 0.055 kips. The maximum load permitted a maximum stress on the uncracked net section of the notch of approximately two-thirds the yield strength of the material. This magnitude of stress was sufficient to produce a visible plastified region at the crack tip. An automatic cycle counter recorded the number of cycles of loading applied.

Since the number of cycles of load range required to initiate a crack from the starter notch was large, several specimens were first precompressed in a standard testing machine to introduce tensile residual stresses at the crack tip. This was accomplished by clamping thick plate blocks on both ends of the specimen to prevent buckling and then applying a compressive load equal in magnitude to two thirds of the tensile load which would be required to produce yielding of the uncracked net section. This loading plastified the region at the tip of the notch and resulted in a residual tensile stress after the compressive load was removed. This operation facilitated the initiation of a crack from the notch. After the crack was started a sufficient number of cycles was applied to grow the crack outside of the plastified region

prior to commencing the crack growth measurements.

Friction grips were used to hold the specimen in the machine as pictured in Fig. 4. Gripping force was applied by uniformly tightening the five bolts on each side of the specimen to a measured torque of 280 in.-lb. The computed mean load (minimum load plus half of the load range) was then statically applied to the specimen. Load range was dynamically applied by initiating vibration of the system.

In most cases an initially high load range was applied to lessen the time needed to start growing a crack from the center notch. After the crack began to propagate from both sides of the notch, the load range was gradually reduced until the desired testing load range was reached. The crack length at this time was considered to be the initial crack length. At this point the selected load range was continuously applied until the test was completed or a runout condition occurred.

Figure 5 shows a close-up view of a typical cracked specimen with the center notch. A fifty-power traveling microscope which can be seen in Fig. 3 was used to follow the propagation of the crack. The end of the notch with the crack emanating from it as viewed through the microscope is seen in Fig. 6. Half crack length was defined as half the distance measured between the crack tip on the right and the crack tip on the left for only one face of the specimen as described in Fig. 7. Since the crack generally does not grow symmetrically with respect to the specimen thickness, and since the crack front is convex in shape the above definition does not give an exact crack length. However, this definition of the half crack length was considered ac-

curate for several reasons:

(1) due to the irregular shape of the crack front no correction to compensate for the shape would necessarily yield an accurate crack length.

(2) in most specimens the crack length on the unmeasured surface (ℓ_{rear}) was less than that on the measured surface (ℓ_{front}), thus compensating for the greater length observed at the leading tip of the convexly curved front (ℓ_{max}).

(3) measurements of all three final crack lengths on the exposed fracture surfaces of several specimens showed a maximum variance of only 1% between the defined crack length (ℓ_{front}) and either of the other two lengths (ℓ_{max},ℓ_{rear}), which appears acceptable for purposes of this study.

4. TEST RESULTS

4.1 Strain Gage Results for Gripping Effect

Since the fabrication process required a shorter specimen than was desired, an investigation was conducted to determine the effect of the short length on the stresses on the notched cross section. Due to the required gripping length of two inches on each end of the specimen only three inches remained between the end of the grip and the notch. Strain gages were mounted at intervals of 3/4 in. over this clear distance as shown in Fig. 8. The gages are located 3/4 in. from the edge of the specimen on each side. Results of taking strain readings at several different static loads indicated that any localized stress caused by gripping had dissipated at the section nearest the grips. The notched cross section did not appear to be affected by the localized gripping stresses.

4.2 Observed Loading Effects

Visible evidence was readily obtained which showed that the material at the crack tip was plastified due to high minimum loads, thus simulating the high residual stresses associated with welded details. At approximately two thirds of the distance from the left of Fig. 6 the crack can be seen to narrow. Also noticeable at this point is a light triangular region extending from the crack to the right at angles of about $\pm$ 45 degrees. This point represents the point at which cycling was stopped and the static mean load was raised from 14.9 kips to 21.0 kips. Such an increase in load pulled apart the section which

was already cracked as is evidenced by the wide initial portion of the crack. The lighter triangular region also gives visible proof that the material near the crack tip was highly plastified. This phenomenon was easily noticed on the fracture surface after the specimen was pulled apart in tension.

Such an exposed fracture surface is pictured in Fig. 9 which shows both surfaces of the crack in specimen CP 28. The interior 40%, which appears smooth, is the notch and the fatigue-cracked portion. The rough areas on each side resulted from the specimen being pulled apart in tension. Bands which appear on the fracture surface clearly indicate the length of the crack at the time the loading scheme was changed. Note especially the thin white lines near the outer portions of the cracked region. This well-defined transition represents the crack length at which one test was terminated and another begun at a higher minimum load but a lower load range.

Figure 10 shows a schematic comparison between the load history and the observed banding of the fracture surface shown in Fig. 9. In this figure the measurements shown in the top cross-section are those distances measured from the centerline to the crack tip on the front surface of the specimen during the actual test. Each dashed region shown indicates the extent of the crack on the front surface at the time the test was temporarily halted to alter the loading. The bottom cross section shows the distances measured from the centerline to the visible banding which was detected on the fracture surface after the test was completed and the specimen was pulled apart in tension.

Good agreement exists for the two sets of measurements made on the front surface of the specimen. It is interesting to note that the initial dark region of crack growth adjacent to the notch abruptly transforms into a lighter region which leads to the initial crack length of the first test -- a_{o_1} (Fig. 9 and Fig. 10). This transition region was due to a high load accidently being applied to the specimen causing the material at the crack tip to plastify. Also from both figures the line which marks the termination of the first test (a_{f_1},a_{o_2}) can clearly be seen. At this point the minimum load was raised and the load range was lowered giving different stress conditions. The affect on the crack growth caused by altering the stresses is shown by the banding.

4.3 Graphic Results

Data was recorded by stopping the test at selected intervals, recording the number of cycles of loading which had been applied, and measuring the overall crack length. In this manner a tabulated record was obtained for the length of the crack after a certain number of cycles of load. These listings are presented in Tables 3 and 4 for all specimens except CP 29 which exhibited no growth at the applied test loads.

As used here N represents the number of cycles of loading required to grow the crack from its initial size to a total length of 2a. Plotting this data in terms of 'a vs. N' yields the typical geometrically increasing relationship shown in Fig. 11. Also shown in Fig. 11 are

the individual half lengths of the crack measured from the centerline of the specimen to the crack tip on each side. This comparison of left and right half lengths shows that crack growth was quite symmetrical.

5. ANALYSIS OF DATA

5.1 Fracture Mechanics Analysis

Fracture mechanics views the crack propagation in terms of its rate of growth, da/dN, and stress intensity at the crack tip, K, which is dependent upon load and geometry. The rate of crack propagation was obtained by computing the slope of the 'a vs. N' curve at each measured value of crack length. A modified difference method[7] was employed to calculate this slope.

The parameters of stress and specimen geometry were expressed in terms of the stress intensity factor for the leading edge of the crack. For the center-notch specimen the stress intensity factor has been expressed by Irwin[8] as

$$K = \sigma\sqrt{\pi a} \tag{1}$$

where σ is the stress on the gross area. For a plate of finite width, W, Irwin has introduced a factor which describes the condition as the crack approaches the edge of the plate as being

$$K = \sigma\sqrt{\pi a}.\sqrt{\sec\left(\frac{\pi a}{W}\right)} \tag{2}$$

Paris and Sih have shown that for short cracks emanating from a circular hole in a plate of infinite width[9]

$$K = \sigma\sqrt{\pi a'} \; . \; f(a'/r) \tag{3}$$

where r is the radius of the hole, a' is the half length minus the hole radius (a'= a-r), and f(a'/r) is some function of the two which approached unity for a >> r. Since fatigue crack propagation is

related to the stress range S_r (or $\Delta\sigma$) to which the crack is subjected, the analysis should be viewed in terms of the range of stress intensity factor ΔK. Thus, the equations describing the stress conditions at the crack tip which produce crack growth in fatigue are

$$\Delta K = S_r\sqrt{\pi a'} \cdot \sqrt{\sec(\pi a/W)} \cdot f(a'/r) \qquad \text{for } a \leq 10r \qquad (4a)$$

$$\Delta K = S_r\sqrt{\pi a} \cdot \sqrt{\sec(\pi a/W)} \qquad \text{for } a > 10r \qquad (4b)$$

for a center-notch plate.

The relationship between rate of propagation and range of stress intensity is shown in the empirical equation proposed for sinusoidal loading[10]

$$da/dN = C\Delta K^n \qquad (5)$$

in which C is a material constant. The value proposed by Paris for the exponent n is 4.0, however, more recent data[11][12][13] suggest a value nearer to 3.0. Expressing the relationship above in the logarithmic form yields the linear relationship

$$\log da/dN = C' + n \log \Delta K \qquad (6)$$

This equation implies that crack growth data when plotted as log da/dN vs. log ΔK should lie along a straight line of slope n which intersects the ordinate at C'. Using the values of $C' = 2.0 \times 10^{-10}$ and n = 3.0 suggested by Hirt and Fisher[14] for welded beams one obtains the straight line shown in Fig. 12. This is a logarithmic plot of da/dN vs. ΔK which also shows the crack propagation data gener-

ated in this investigation. Note the general tendency of the data to follow the beam data line except in the region of very slow growth ($da/dN < 10^{-8}$ in/cycle). This is the area of crack growth which corresponds to extreme life conditions in most structural details ($N > 10^7$ cycles). It is interesting to note that along with the specimens which showed measured crack growth, two specimens displayed no growth for about 20 million cycles of load application. The ΔK values corresponding to these two specimens are shown as solid points in Fig. 12.

5.2 Comparison with Complementary Crack Growth Investigation

Low cycle fatigue crack growth studies have been conducted previously on center-notch specimens fabricated from the same rolled plate material which was used in this investigation.[13] The data from this low cycle study is plotted in Fig. 13 along with the same crack propagation line and data from Fig. 12. This low cycle data represents the final phase of crack growth in which the stresses on the net section reach and exceed the yield strength of this material due to either high stress or large crack lengths. Thus the combined data provide a complete description of the fatigue crack propagation in A36 plate material. It is to be noted that the data in the upper portion of the graph ($da/dN > 10^{-6}$ in./cycle) also show a tendency to deviate from the welded beam crack propagation line. There appears to be three distinct phases of fatigue crack propagation which are highly dependent on the range of stress inten-

sity and material properties. This observed phenomenon substantiates the trend of three-phase fatigue crack propagation determined elsewhere.[16][17]

5.3 Threshold and High Cycle Fatigue

It has been determined that the critical region of fatigue crack growth for welded structural details is below 10^{-6} in./cycle.[14] Of the total life required to grow a crack from its initial size to a visible crack, more than 75% was consumed in this region. Since this study deals with high cycle and threshold fatigue crack growth the final brief phase of crack growth above 10^{-6} in/cycle will not be examined.

Threshold fatigue crack propagation appears to occur at about 10^{-8} in./cycle at ΔK levels between 3.3 and 5.3 ksi $\sqrt{\text{in.}}$ in Fig. 13. This level agrees with that found by Paris for AISI 9310 steel.[15] Thus the region of crack propagation below 10^{-8} in./cycle was considered to be the threshold area as shown in Fig. 14. In this region it can be seen that crack growth is extremely slow or nonexistent. The region designated as low cycle fatigue is the final phase of rapid crack growth as described above. Of interest to most structural engineers is the high cycle fatigue region which represents the fatigue region in which most structural failures originate.

A standard linear regression analysis was performed on all data generated from both studies which was contained in the high cycle fatigue region in Fig. 14. The mean line and confidence limits for the 95% interval are shown as the solid line and dashed

lines respectively. Noting the equation of the mean line

$$da/dN = 9.80 \times 10^{-11} \Delta K^{3.1} \qquad (7)$$

it is seen that good agreement exists with the equation proposed for welded beams.[14]

In the threshold region a vertical scatter-band has been drawn to include all points which indicate threshold fatigue crack growth. The limiting values of ΔK for this interval are 3.3 and 5.2 ksi - $\sqrt{in.}$ Harrison suggested a threshold value for mild steel of $\Delta K/E = 1.16 \times 10^{-4} \sqrt{in.}$ which provides a $\Delta K = 3.4$ ksi $\sqrt{in.}$[18] In his investigation on 9310 steel Paris observed a tendency towards a threshold value of $\Delta K = 5.1$ ksi $\sqrt{in.}$ These two values correspond closely to the observed limiting values of the threshold region shown in Fig. 14. Averaging the two values of ΔK which showed no crack growth also yields a threshold value of 3.3. ksi $\sqrt{in.}$ Evidence indicates that a fatigue crack propagation level does exist in the range of $\Delta K = 3 - 5$ ksi $\sqrt{in.}$

5.4 Effect of Minimum Stress

Minimum stress, in terms of the stress intensity factor, has been observed to have some influence on fatigue crack growth in both the threshold and high cycle regions.[15] When the minimum stress was an order of magnitude larger than the stress range, significantly lower values of stress intensity range produced the same growth rates that resulted from the minimum stress and stress range being

the same order of magnitude. This phenomenon was not confidently observed in this study. As can be seen in Fig. 15 when one reflects the stress parameters in terms of stress intensity the normal scatter of data overshadows any distinguishable effects. Comparing specimens CP 26-1, CP 26-2, and CP 27 one notes that all three have initially the same range in stress intensity. Specimens CP 26-1 and CP 27 also have approximately the same initial minimum stress intensity factor. Clearly these specimens exhibit considerable scatter with CP 27 showing a tendency toward threshold. Specimen CP 26-2 has a minimum stress intensity which is approximately twice that of the other two yet it agrees in part with each and also shows a tendency toward threshold.

Other evidence indicating no significant effect of minimum stress can be seen in phases 1 and 2 of specimen CP 28. Both have approximately the same initial range in stress intensity, but a large difference exists in initial minimum stress intensity. Close agreement exists, however, for the two sets of data over the range tested. No distinguishable effect of minimum stress can be claimed from this investigation. This agrees with the findings of the low cycle fatigue study performed on these same specimen types.[13]

5.5 Correlation With Coverplated Beam Studies

Hirt and Fisher demonstrated how the fatigue crack threshold stress intensity range could be used to predict the runout value of stress range for welded beams.[14] By employing a crack model to cor-

relate the beam detail with the threshold value of a crack propagation specimen this prediction is easily attainable. This approach requires an accurate model to describe the stress intensity for the particular geometrical situation being investigated. In this study the cover plate welded to the beam flange was the detail chosen since it represents the most critical fatigue crack propagation situation of common welded details.

The mathematical model used to describe the stress intensity factor at the toe of fillet welds was suggested in Ref. 5 based on studies reported in part in Ref. 6. This condition is shown in Fig. 16 as it exists in the end-welded cover-plated beam. In this case the surface crack which exists at the weld toe is assumed to have a semi-elliptical shape. Irwin has shown that the stress intensity factor for this crack configuration when embedded in an infinite plate is [19]

$$K = \sigma\sqrt{\pi a} \cdot \left[\frac{1 + 0.12\ (1-a/b)}{\Phi_o}\right] \qquad (8)$$

where a is the depth of the crack, b is the crack width, and Φ_o is an elliptical integral that depends on the ratio a/b. Describing the entire semi-elliptical correction function as q(a/b) and combining Equation 8 with the secant correction for finite plate thickness one can model the stress concentration factor at a weld toe crack as

$$K = K_T \cdot \sigma_{fl} \cdot g(a/t') \cdot q(a/b) \cdot \sqrt{\pi a} \cdot \sqrt{\sec(\pi a/2t')} \qquad (9) \ .$$

Here K_T is the stress concentration factor for the weld toe, σ_{fl} is the stress in the flange, t' is the thickness of the flange, and g(a/t') is a decay function which describes the dissipation of the stress concentration effect as the crack progresses through the flange. Frank described this decay function in polynomial form as [6]

$$g(a/t') = 1 - 3.215\ (a/t') + 7.897(a/t')^2 - 9.288(a/t')^3 + 4.086(a/t')^4 \qquad (10)$$

When Equation 8 is written in terms of the range of the stress intensity factor it can be related to the growth rate by Equation 5

$$da/dN = C\ .\ [\Delta\sigma_{fl}\ .\ K_T\ .\ g(a/t')\ .\ q(a/b)\ .\ \sqrt{\pi a.\sec(\pi a/2t')}]^n \qquad (11)$$

Rearranging Equation 11 for purposes of integration yields

$$dN = 1/C\ .\ \frac{da}{[\Delta\sigma_{fl}.K_T.g(a/t').q(a/b).\sqrt{\pi a.\sec(\pi a/2t')}]^n} \qquad (12)$$

Integrating over the interval from a_o to a_f gives the following relationship:

$$N = \frac{1}{C[\Delta\sigma_{fl}.K_T]^n} \cdot \int_{a_o}^{a_f} \frac{da}{[g(a/t').q(a/b).\sqrt{\pi a.\sec(\pi a/2t')}]^n} \qquad (13)$$

which defines the fatigue life of the detail for various crack sizes. In this equation many variables appear to be unknown. However, a mean regression relationship has been developed expressing the total fatigue life of cover-plated beams in terms of the induced stress range as [1]

$$\log N = 9.292 - 3.095 \log S_r \qquad (14)$$

Thus, for selected stress ranges, N can be determined from Equation 14 and both N and S_R can be substituted into Equation 13 which is rearranged to define K_T as

$$K_T = \frac{1}{S_r[C.N]^{1/n}} \left\{ \int_{a_o}^{a_f} \frac{da}{[g(a/t').q(a/b).\sqrt{\pi a}.\sec(\pi a/2t')]^n} \right\}^{1/n} \qquad (15)$$

The final crack size can be taken as the flange thickness since over 95% of the life of the detail is consumed growing the crack from its initial size through the flange.[20] Signes, et al. measured common flaw sizes inherent in fillet-welded details.[21] Studies on beams with transverse stiffeners indicated the probable existence of the same initial flaw sizes at weld toe terminations.[5] A mean initial flaw size of 0.003 in. was obtained and applied to the cover-plated beam situation. When this initial flaw size was used in Equation 15 it yielded a stress concentration factor of $K_T = 4.45$ for the cover-plated beam.

Assuming this value correctly describes the stress concentration at the toe of the fillet weld connecting the cover plate to the beam flange, one can evaluate the "runout" stress range. Equation 9 was used to determine the stress range as

$$S_{r_{runout}} = \frac{\Delta K}{K_T} \cdot \frac{1}{g(a/t') \cdot q(a/b).\sqrt{\pi a}.\sec(\pi a/2t')} \qquad (16)$$

Choosing the threshold value $\Delta K = 3.3$ ksi $\sqrt{\text{in.}}$ found previously and the initial crack sizes suggested in Reference 5 permits the threshold stress range to be evaluated. By determining the runout stress range in this manner one views the problem as being dependent only on the

initial flaw size. The stress concentration factor is assumed constant for all initial flaw sizes, and no influence of minimum stress is assumed to exist.

Figure 17 shows the three runout values obtained when the initial crack size is assumed to be the values obtained for transverse stiffeners.[5] These values of 0.001 in. (upper limit),0.003 in. (mean size), and 0.020 in. (lower limit) were compatible with the measured values at weld toes.[21] Also shown in this figure are the results of 204 coverplated beams tested previously[1] and 9 coverplated beams tested in conjunction with this study. It can be seen that a wide range exists for the predicted runout values of stress range over the scatter of initial flaw sizes varying from 0.001 in. to 0.020 in. The lower bound provided by the largest initial flaw size is in reasonable agreement with the test data.

Since the runout stress range was determined from a threshold value of stress intensity range it can be expected that only the larger flaws will propagate to failure under threshold conditions. Hence under low cyclic stress ranges, no cracks will propagate from flaw sizes less than the largest observed flaw size in the weld. This trend is also shown by the data. The two data points at the 8 ksi stress range level probably had smaller than average initial flaw sizes. Testing was discontinued before any visible cracking was observed.

Initial flaw sizes of fillet welds have been shown to be greatly dependent upon welding techniques.[21] Therefore, beams with similar welded details can be expected to exhibit marked differences in fatigue life. These differences could be greatly pronounced in the vicinity

of the runout stress range at the fatigue crack growth threshold. Figure 17 shows the widening range of fatigue lives for the lower stress ranges.

This study has shown that basic crack growth data in the threshold region can be used to estimate the expected fatigue life of actual structural details. Hence, estimates of the threshold level can be made for other types of structural details which have experienced fatigue damage in the field.

6. CONCLUSIONS

This investigation provides pertinent data for the area of threshold fatigue crack propagation. More importantly this data was employed to predict a runout region of stress range for an actual structural detail. Following are the most notable findings of this study.

1. The localized effect of the friction grips was confined to a very short distance from the end of the grips. Therefore relatively short specimens were permissable without jeopardizing the desired stress conditions in the vicinity of the center notch.

2. Upon examination of several fracture surfaces it was discovered that several distinct regions of crack growth existed. The distances of these regions from the center of the specimen coincided with recorded surface cracks at changes of loading. Some distinct markings of the surface also coincided with crack lengths at which cycling was halted overnight. It was found that the markings on the fracture surface provide an accurate record of both the static and cyclic load histories of the specimen.

3. Linear elastic mechanics provides a good description of the crack propagation behavior of A36 steel. It provides a valuable tool to understand the stress conditions and fatigue crack problem in structural details.

4. A36 steel exhibits three distinct regions of fatigue crack propagation. These regions can be described as threshold growth, high cycle fatigue, and low cycle fatigue. Structural fatigue design considers the threshold and high cycle fatigue regions. Where extreme amounts of cyclic loading occurs the threshold growth is of major concern.

5. A36 steel exhibits a threshold range of the stress intensity factor. For the long life studies conducted two specimens with relatively large cracks showed no crack propagation after 17-20 million cycles. The average threshold value of stress intensity range for these specimens was $\Delta K = 3.3$ ksi $\sqrt{in}$. Threshold growth observed in other specimens confirmed this value as a lower bound for the threshold region.

6. For all phases of crack propagation the range of stress intensity was shown to be the major influencing stress variable. This finding agrees with studies on welded details which also indicate that stress range is the dominant stress variable affecting fatigue life in structural details. No discernible influence of the minimum stress variable was evident considering the scatter of the data.

7. Fracture mechanics analysis allows a threshold stress intensity factor range to be developed which is useful in predicting stress

ranges which cause no noticeable fatigue crack growth in structural details. By modelling the stress conditions for a particular welded detail, the cover-plated beam, a runout stress range of S_r = 4.6 ksi was predicted for an assumed initial flaw of 0.020 in. Beam studies now in progress on this detail tend to confirm this predicted value.

8. Wide ranges of runout stress range can exist due to the different sizes of observed initial flaws. The large variation of failure life noticed for details tested at the lower stress ranges tends to confirm this.

NOMENCLATURE

a	= average half length of crack; depth of semi-elliptical crack.
b	= width of semi-elliptical crack.
a_o	= initial half length of crack.
a_f	= final half length of crack.
a'	= actual length of crack emanating from circular hole = a-r.
C	= material constant in crack growth equation.
C'	= log C.
da/dN	= rate of growth of the crack.
E	= Young's modulus of elasticity.
$f(a'/r)$	= mathematical function of crack length and circular hole radius.
$g(a/t')$	= decay function for stress concentration influence.
K	= elastic stress intensity factor for the leading edge of a crack.
ΔK	= range of the stress intensity factor.
K_{min}	= minimum stress intensity factor.
K_T	= stress concentration factor.
L	= length of the specimen.
ℓ_{front}	= distance between the two leading crack edges as measured at the front surface of the specimen.
ℓ_{max}	= distance between the two foremost portions of the leading crack edges as measured over the interior fracture surface.
ℓ_{rear}	= distance between the two leading crack edges as measured at the rear surface of the specimen.
N	= number of cycles of applied loading; number of cycles to failure in welded beam details.

n = exponent in crack growth equation.

$q(a/b)$ = semi-elliptical correction factor.

r = radius of center hole in specimen.

S_r, $\Delta\sigma$ = range of stress on the gross area.

t' = thickness of the beam flange.

W = width of the specimen.

σ = stress on the gross area of the specimen.

σ_{cp} = stress transferred into the cover plate.

σ_{fl} = stress in the flange at a distance from the cover plate.

σ'_{fl} = stress remaining in the flange under the cover plate.

$\Delta\sigma_{fl}$ = range of stress in the flange.

Φ_o = elliptical integral.

TABLE 1

MATERIAL PROPERTIES OF 3/8" A36 ROLLED PLATE

	Tensile Coupons			
	1	2	3	Average
Dynamic Yield Strength (ksi)	36.7	37.1	35.8	36.5
Static Yield Strength (ksi)	34.6	33.3	34.9	34.3
Ultimate Strength (ksi)	60.2	60.5	60.0	60.2
Per Cent Elongation	27.0	27.8	28.3	27.7
Per Cent Reduction in Area	45.6	47.3	44.9	45.9

TABLE 2

MATERIAL PROPERTIES OF ROLLED A36 FLANGE

	Tensile Coupons				
	1	2	3	4	Average
Dynamic Yield Strength (ksi)	41.1	37.1	38.4	39.5	39.0
Static Yield Strength (ksi)	39.2	31.4	34.4	37.5	35.6
Ultimate Strength (ksi)	62.8	60.2	61.8	60.3	61.3
Per Cent Elongation	28.3	27.9	26.5	29.2	28.0
Per Cent Reduction in Area	46.4	45.3	46.8	52.7	47.8

TABLE 3

CRACK GROWTH DATA FOR CENTER-NOTCHED SPECIMENS FROM A36 STEEL PLATE

SPECIMEN CP 23 AVERAGE

MINIMUM LOAD= 2.0 KIPS

LOAD RANGE= 8.4 KIPS

A (IN.)	N (CYCLES)
.2069	0.
.2913	3572000.
.3379	4221000.
.3676	4697000.
.4136	5262000.
.4828	5922000.
.4912	5998000.
.6037	6570000.
.7249	7018000.
1.0613	7518000.
1.1932	7617000.
1.3283	7669000.

SPECIMEN CP 24 AVERAGE

MINIMUM LOAD= 10.3 KIPS

LOAD RANGE= 6.2 KIPS

A (IN.)	N (CYCLES)
.2917	0.
.3942	1446000.
.4124	1573000.
.4726	2365000.
.5341	2835000.
.6070	3250000.
.7176	3810000.
1.0393	4898000.
1.1094	5002000.

TABLE 3 (continued)

SPECIMEN CP 25 AVERAGE

MINIMUM LOAD= 2.0 KIPS

LOAD RANGE= 6.2 KIPS

A (IN.)	N (CYCLES)
.2938	0.
.3064	720000.
.3231	1690000.
.3332	2850000.
.3548	4130000.
.3930	6002000.
.4274	7130000.
.4625	8090000.
.4966	8760000.
.5282	9410000.
.5633	9921000.
.6094	10560000.
.6549	11080000.
.7041	11540000.
.7532	11930000.
.8199	12380000.
.8835	12720000.
.9696	13090000.
1.0632	13380000.

SPECIMEN CP 27 AVERAGE

MINIMUM LOAD= 14.5 KIPS

LOAD RANGE= 5.3 KIPS

A (IN.)	N (CYCLES)
.2899	0.
.2912	872000.
.3001	1640000.
.3120	2440000.
.3384	3740000.
.3534	4540000.
.3698	5340000.
.3896	6140000.
.4109	6940000.
.4323	7740000.
.4565	8440000.
.4792	9190000.
.5036	9890000.
.5154	10190000.

TABLE 3 (continued)

SPECIMEN CP 26-1 AVERAGE

MINIMUM LOAD= 14.5 KIPS

LOAD RANGE= 6.2 KIPS

A (IN.)	N (CYCLES)
.2074	0.
.3076	2935000.
.3429	3525000.
.3567	3770000.
.3626	3840000.
.3641	3870000.
.3952	4230000.
.4903	5172000.
.5638	5776000.
.6351	6224000.
.7086	6674000.

SPECIMEN CP 26-2 AVERAGE

MINIMUM LOAD= 15.0 KIPS

LOAD RANGE= 3.1 KIPS

A (IN.)	N (CYCLES)
.7086	0.
.7145	450000.
.7426	1081000.
.7487	1928000.
.7657	2670000.
.7827	3413000.
.7977	4065000.
.8181	4875000.
.8402	5611000.
.9244	7217000.
1.0025	8104000.
1.0598	8755000.
1.0934	9023000.

TABLE 3 (continued)

SPECIMEN CP 28-1 AVERAGE

MINIMUM LOAD= 13.4 KIPS

LOAD RANGE= 3.1 KIPS

A (IN.)	N (CYCLES)
.4020	0.
.4086	2016000.
.4157	4537000.
.4215	6537000.
.4321	8537000.
.4442	10537000.
.4565	12537000.
.4652	14037000.
.4757	15607000.
.4901	17237000.
.4996	18607000.

SPECIMEN CP 28-2 AVERAGE

MINIMUM LOAD= 19.6 KIPS

LOAD RANGE= 2.8 KIPS

A (IN.)	N (CYCLES)
.4996	0.
.5162	1800000.
.5262	3200000.
.5339	4600000.
.5422	6100000.
.5553	7230000.
.5652	8400000.
.5789	9500000.
.5961	10950000.
.6094	11950000.
.6194	13000000.
.6381	14200000.
.6641	15450000.
.6748	16050000.

TABLE 4

CRACK GROWTH DATA FOR CENTER-NOTCHED SPECIMENS FROM

A36 STEEL BEAM FLANGE

SPECIMEN CF 1 AVERAGE

MINIMUM LOAD= 22.2 KIPS

LOAD RANGE= 3.1 KIPS

A (IN.)	N (CYCLES)
.2379	0.
.2384	2500000.
.2398	4000000.
.2412	5600000.
.2424	6800000.
.2444	9100000.
.2500	11100000.
.2528	12600000.
.2551	14800000.
.2614	16800000.
.2668	18250000.
.2724	20250000.
.2818	22380000.
.2900	24050000.
.2948	25550000.
.3050	27050000.
.3103	28550000.
.3169	29750000.
.3235	31250000.

TABLE 5

THRESHOLD VALUES OF STRESS INTENSITY RANGE

a. Specimens in which growth was observed

Spec	Type	Lowest ΔK at growth (ksi-$\sqrt{in.}$)	K_{min} at growth (ksi-$\sqrt{in.}$)	Growth rate at lowest ΔK (in./cycle)
CP 23	Plate	7.2	1.7	2.36×10^{-8}
CP 24	"	6.4	10.6	7.09×10^{-8}
CP 25	"	6.4	2.1	1.76×10^{-8}
CP 26-1	"	5.3	12.5	3.41×10^{-8}
CP 26-2	"	5.4	26.2	1.32×10^{-8}
CP 27	"	5.4	14.8	1.38×10^{-9}
CP 28-1	"	3.7	16.1	3.30×10^{-9}
CP 28-2	"	3.8	26.9	9.25×10^{-9}
CP 29*	"	3.8	20.9	4.85×10^{-10}
CF 1	Flange	3.3	23.5	2.20×10^{-10}

b. Specimens in which no growth was observed

Spec.	Type	Highest ΔK at no growth (ksi-$\sqrt{in.}$)	K_{min} at no growth (ksi-$\sqrt{in.}$)	Number of cycles for runout
CP 29	Plate	3.6	20.6	17,000,000
CF 1	Flange	3.0	28.2	20,000,000

*only two points -- da/dN is slope of straight line between the points.

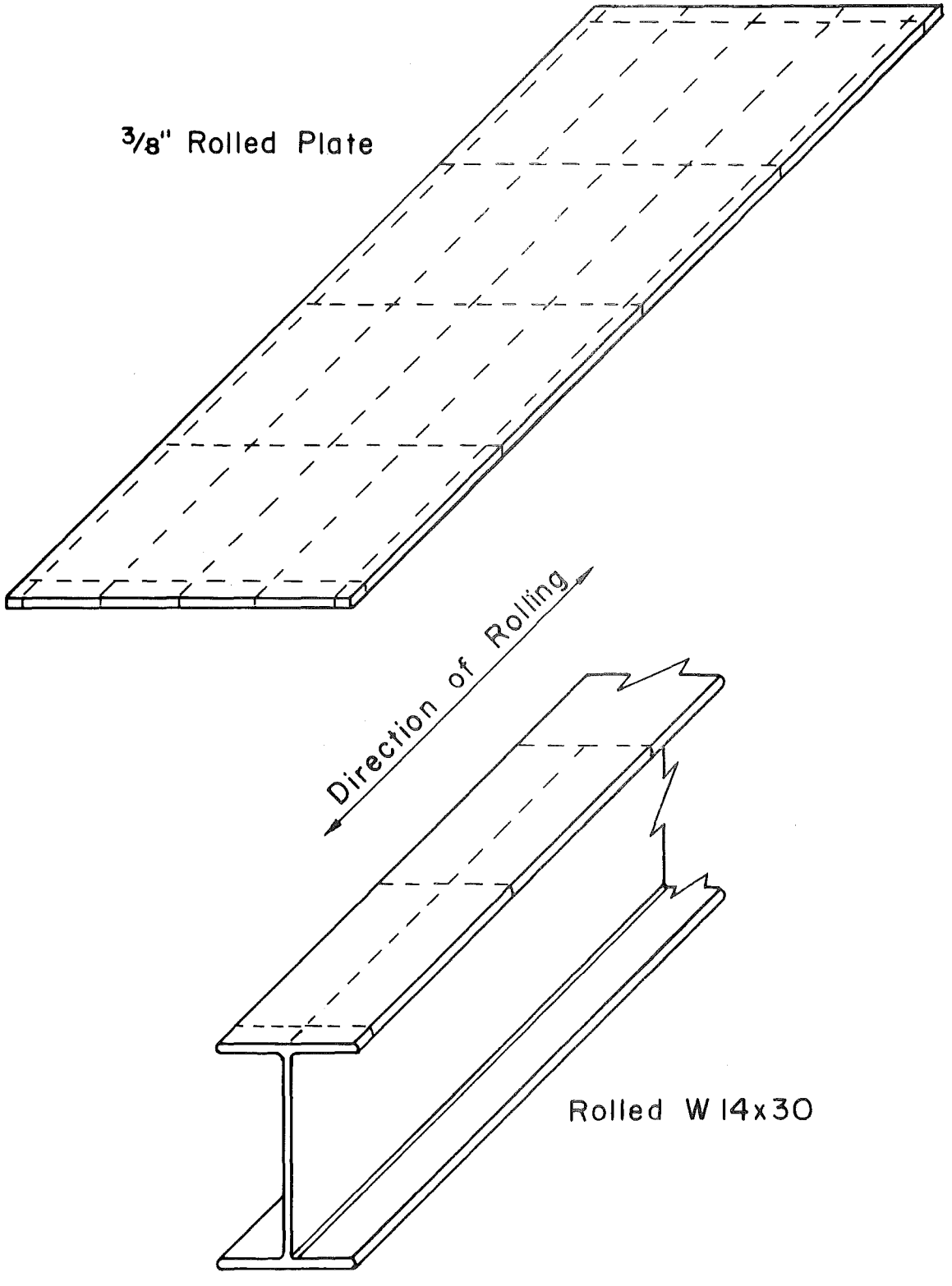

Fig. 1 Origin of Specimens

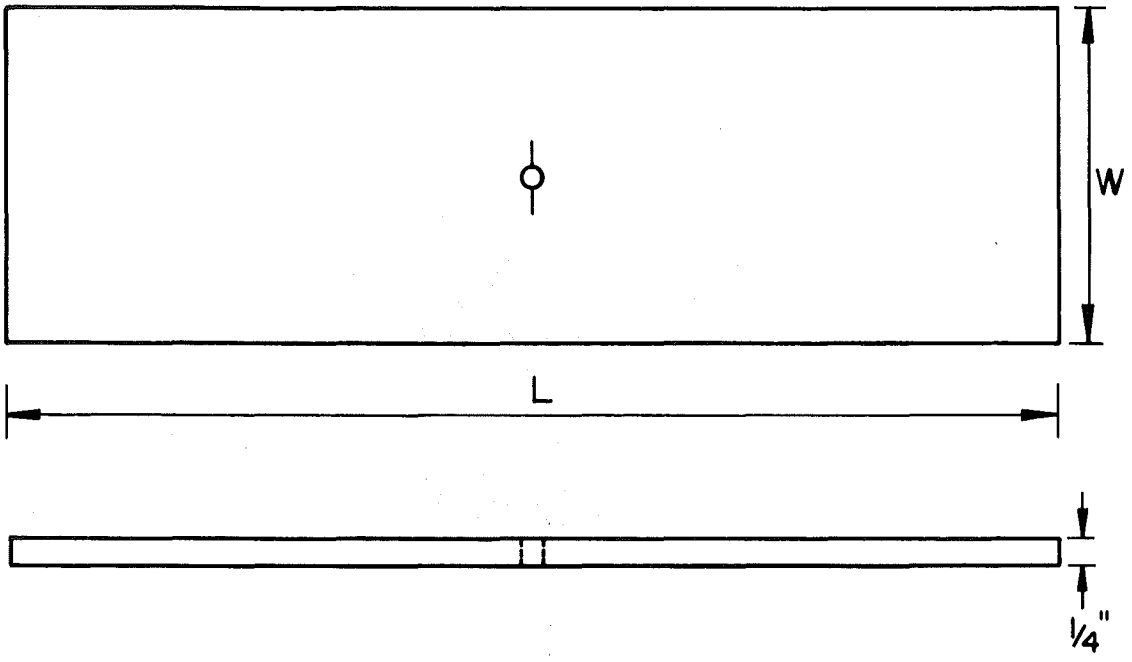

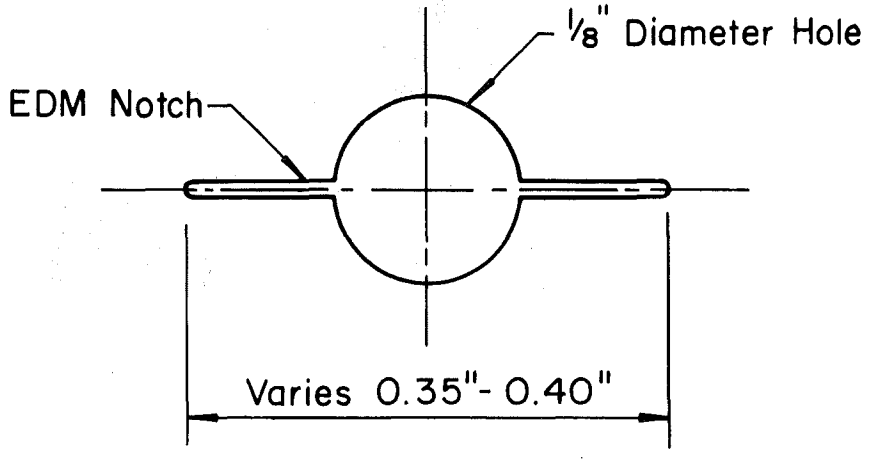

Fig. 2 Geometry of Specimen and Center Notch

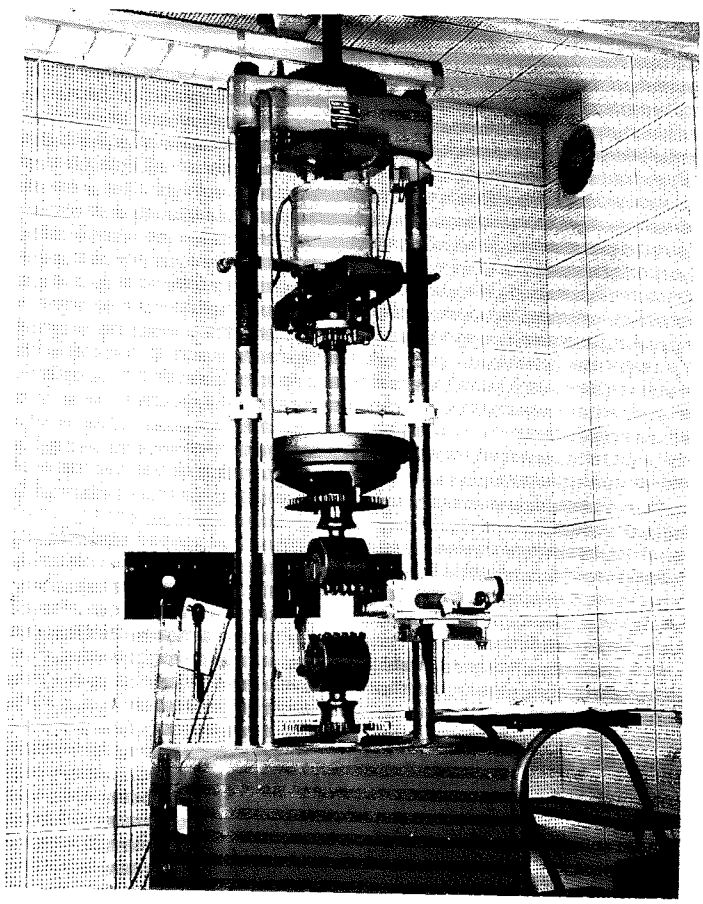

Fig. 3 Specimen Mounted in Testing Machine

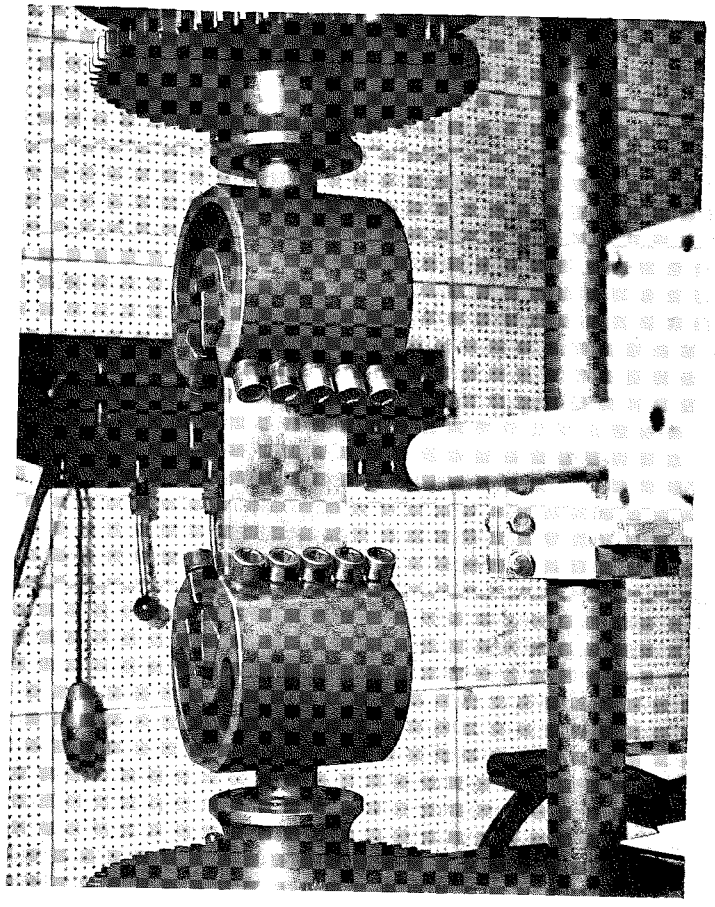

Fig. 4 Close-up of Specimen in Grips

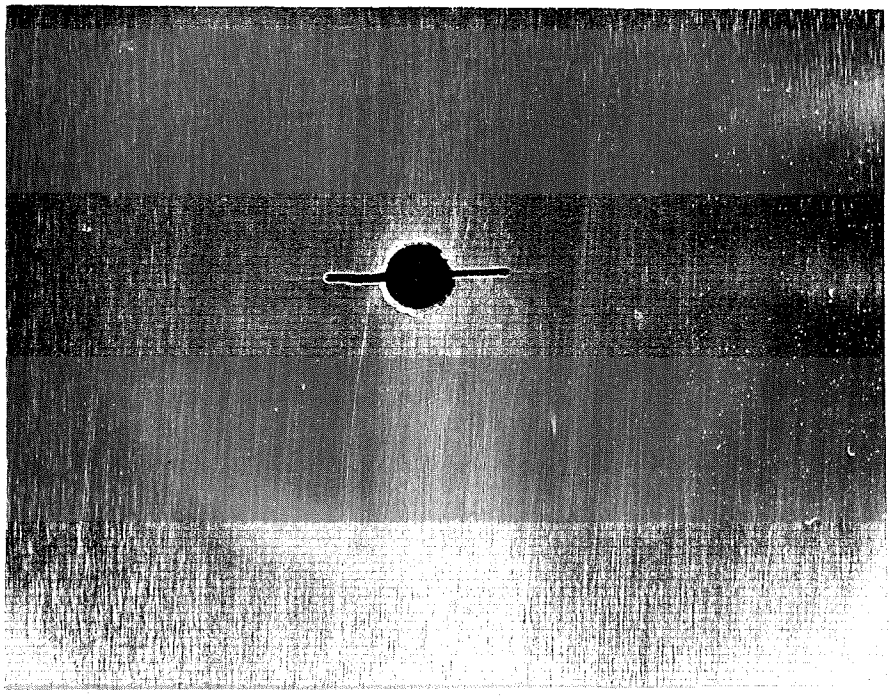

Fig. 5 Cracks Emanating from Center Notch

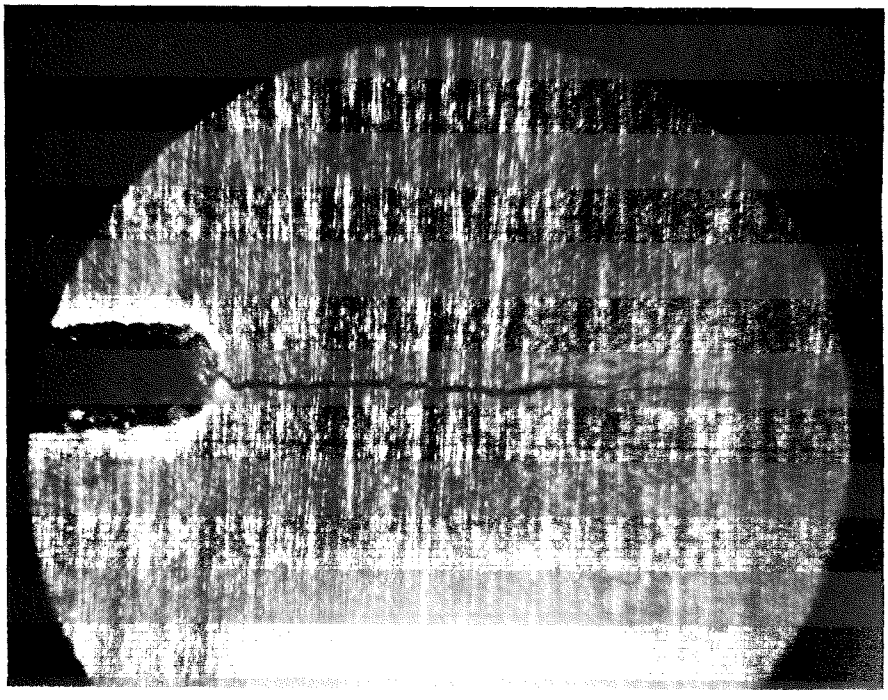

Fig. 6 Notch Tip and Crack Viewed Through Microscope

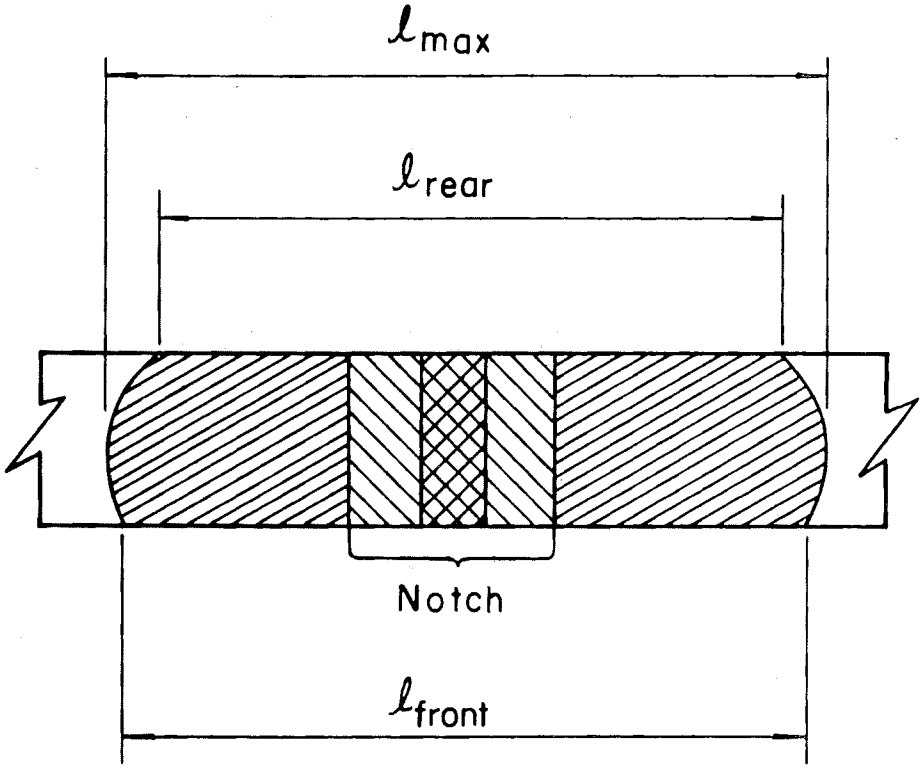

Fig. 7 Crack Length Defined on Fracture Surface

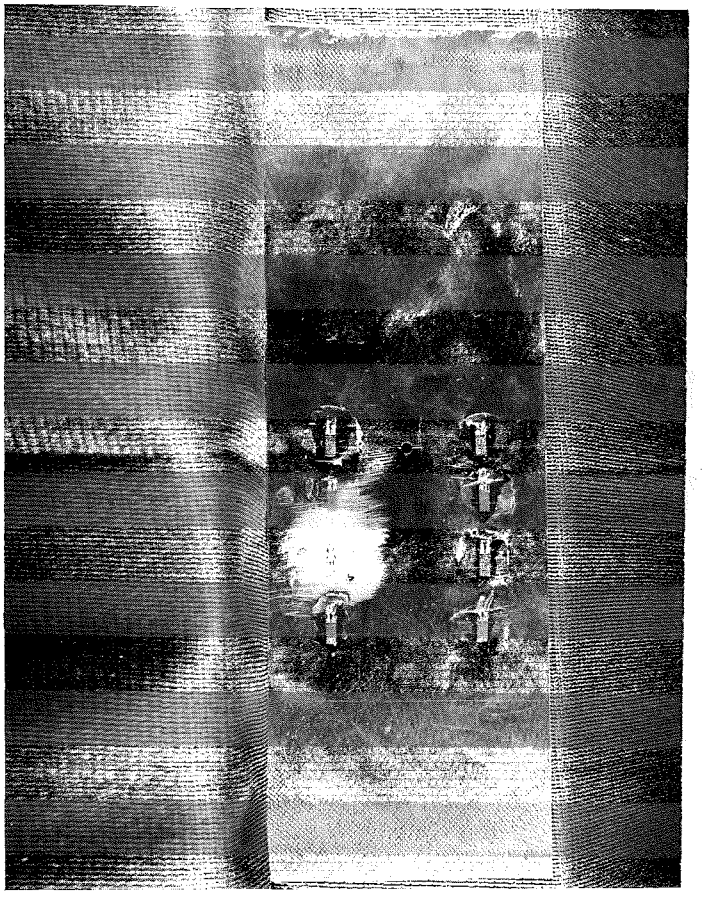

Fig. 8 Strain Gages Mounted on Specimen

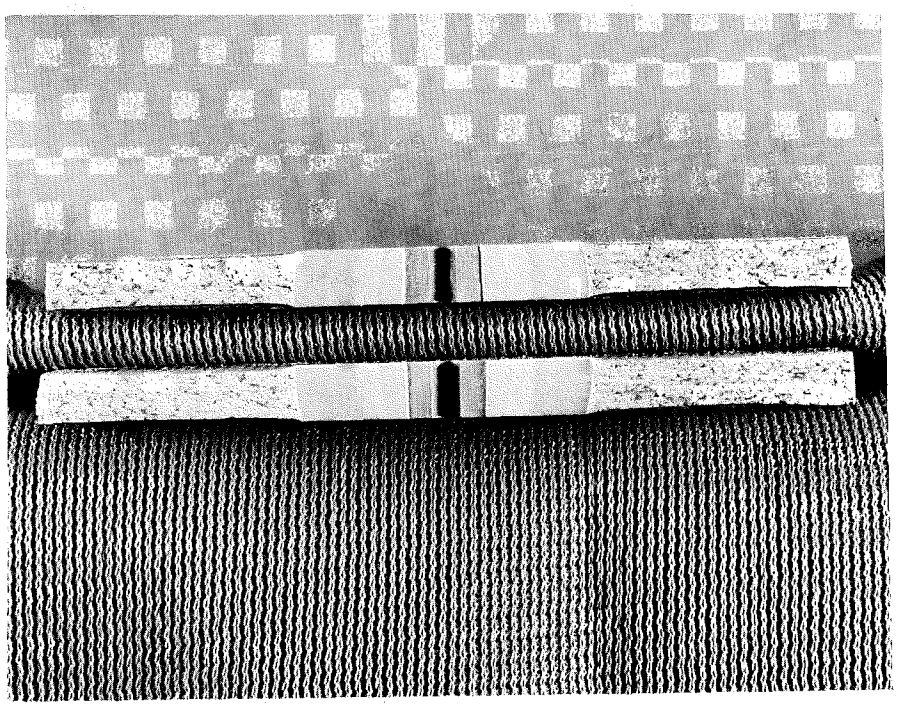

Fig. 9 Typical Exposed Fracture Surface

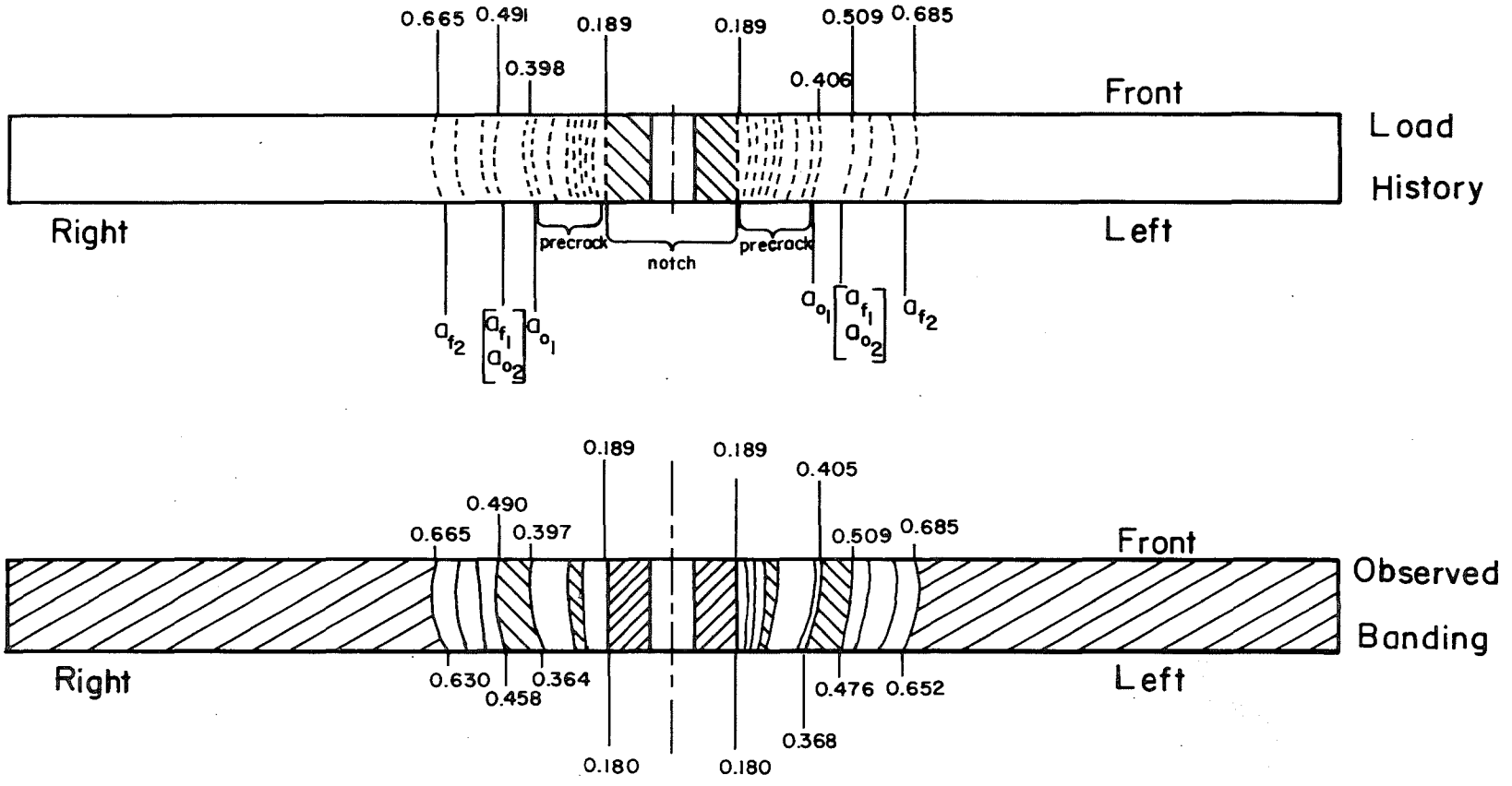

Fig. 10 Comparison of Load History and Observed Banding

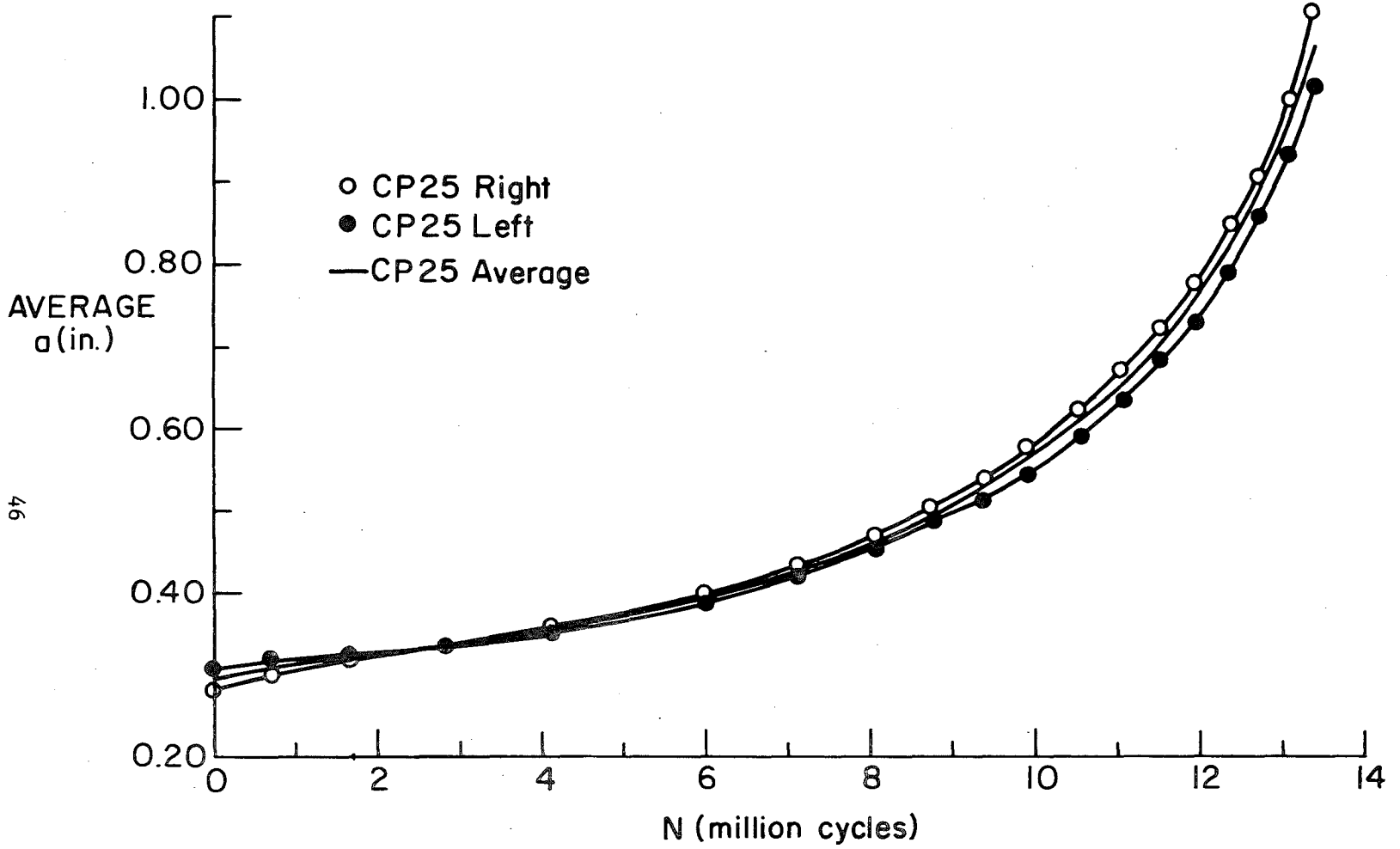

Fig. 11 Typical a vs. N. Plot Comparing Average, Left, and Right Crack Sizes

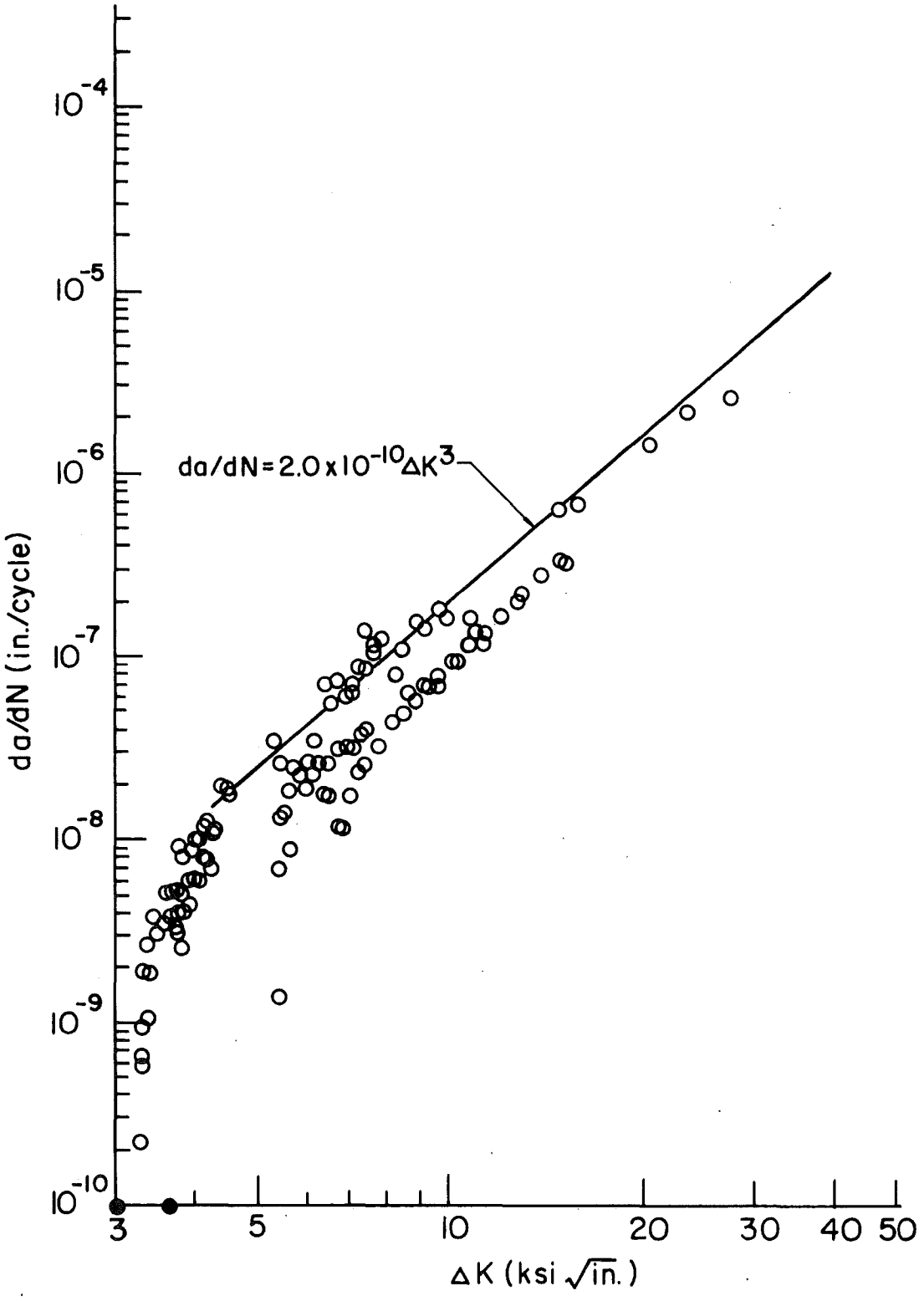

Fig. 12 Crack Propagation Data and Mean Line for Welded Beams

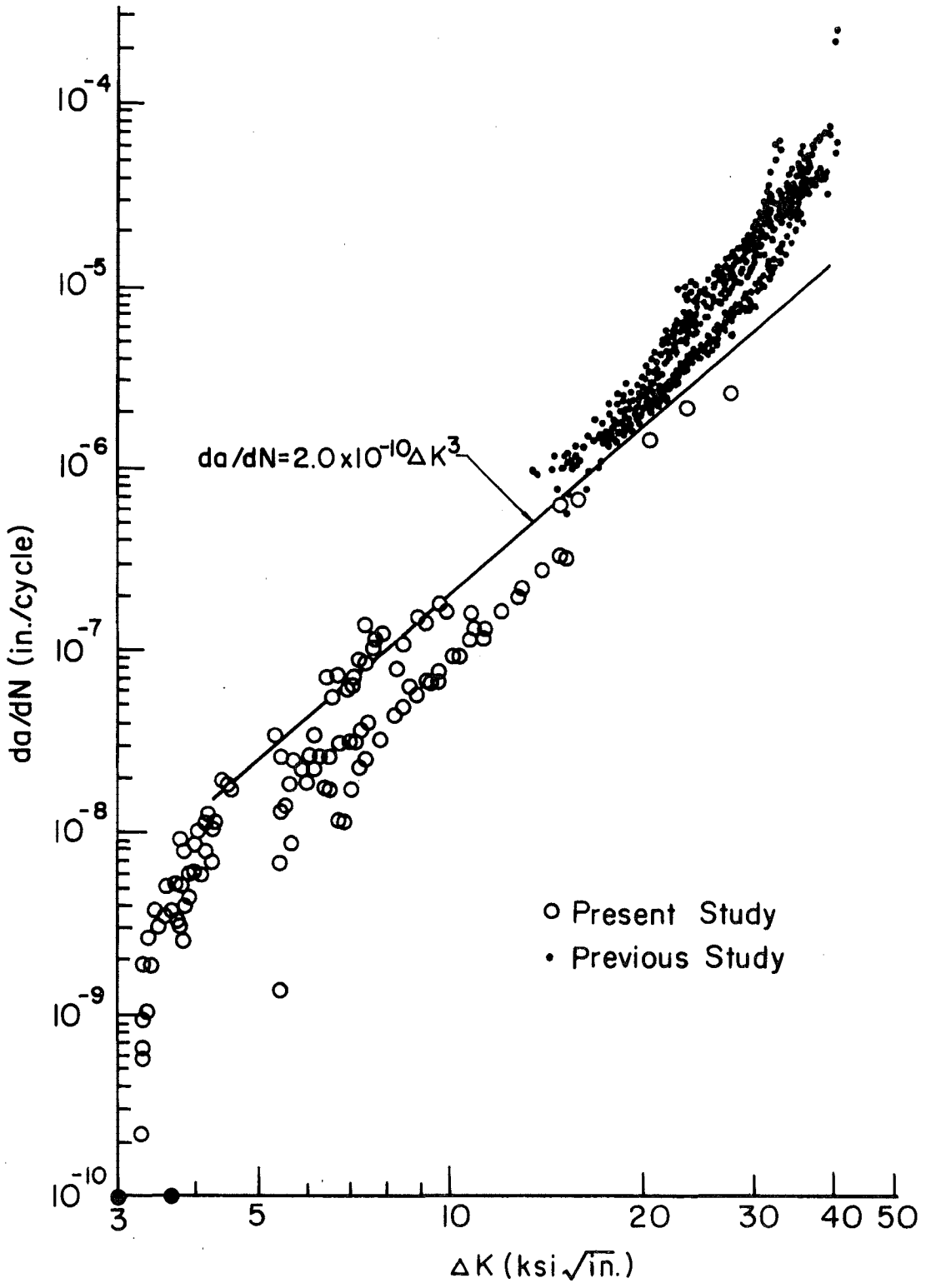

Fig. 13 Summary of Fatigue Crack Growth for A36 Steel

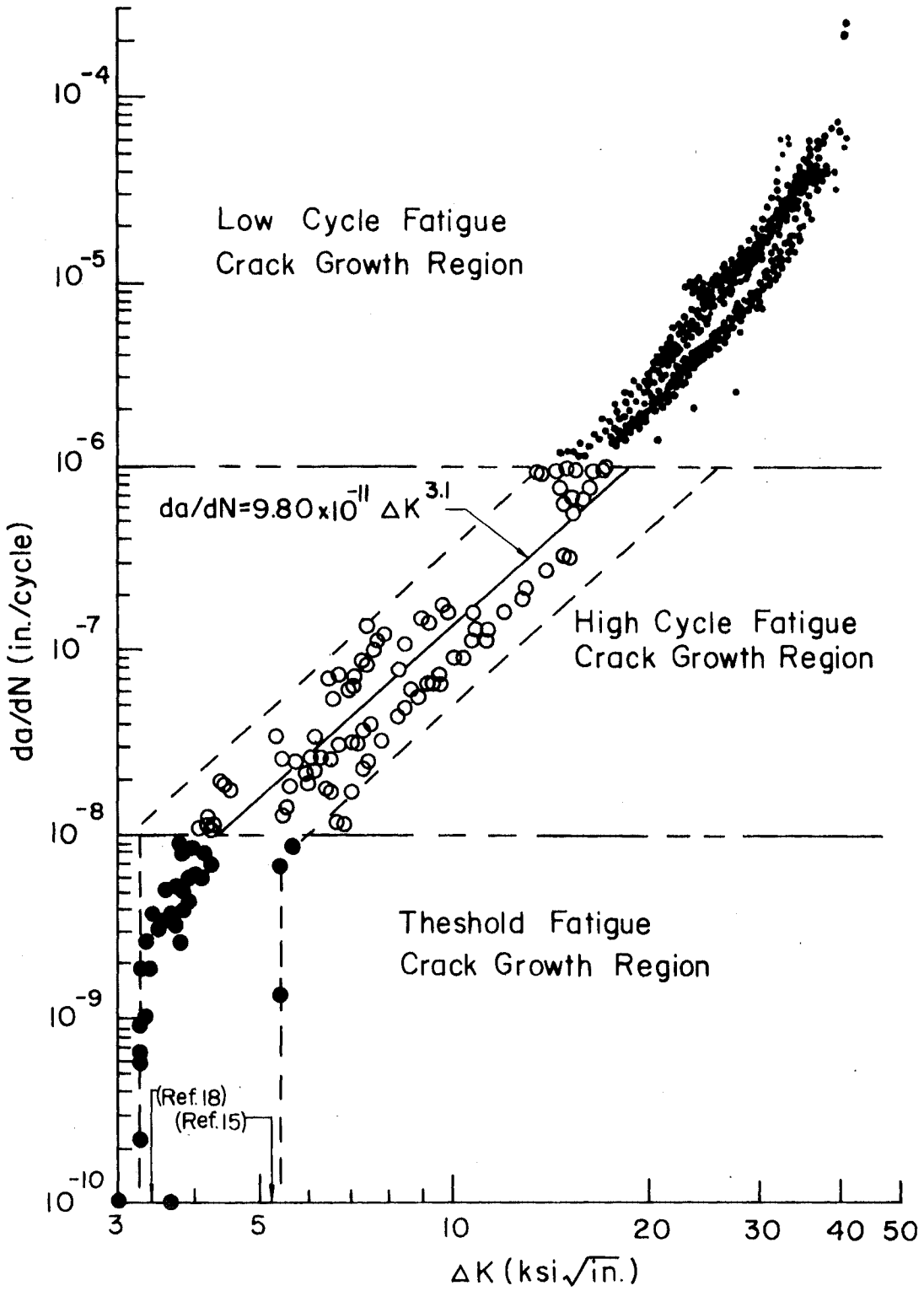

Fig. 14 Critical Regions of Fatigue Crack Propagation

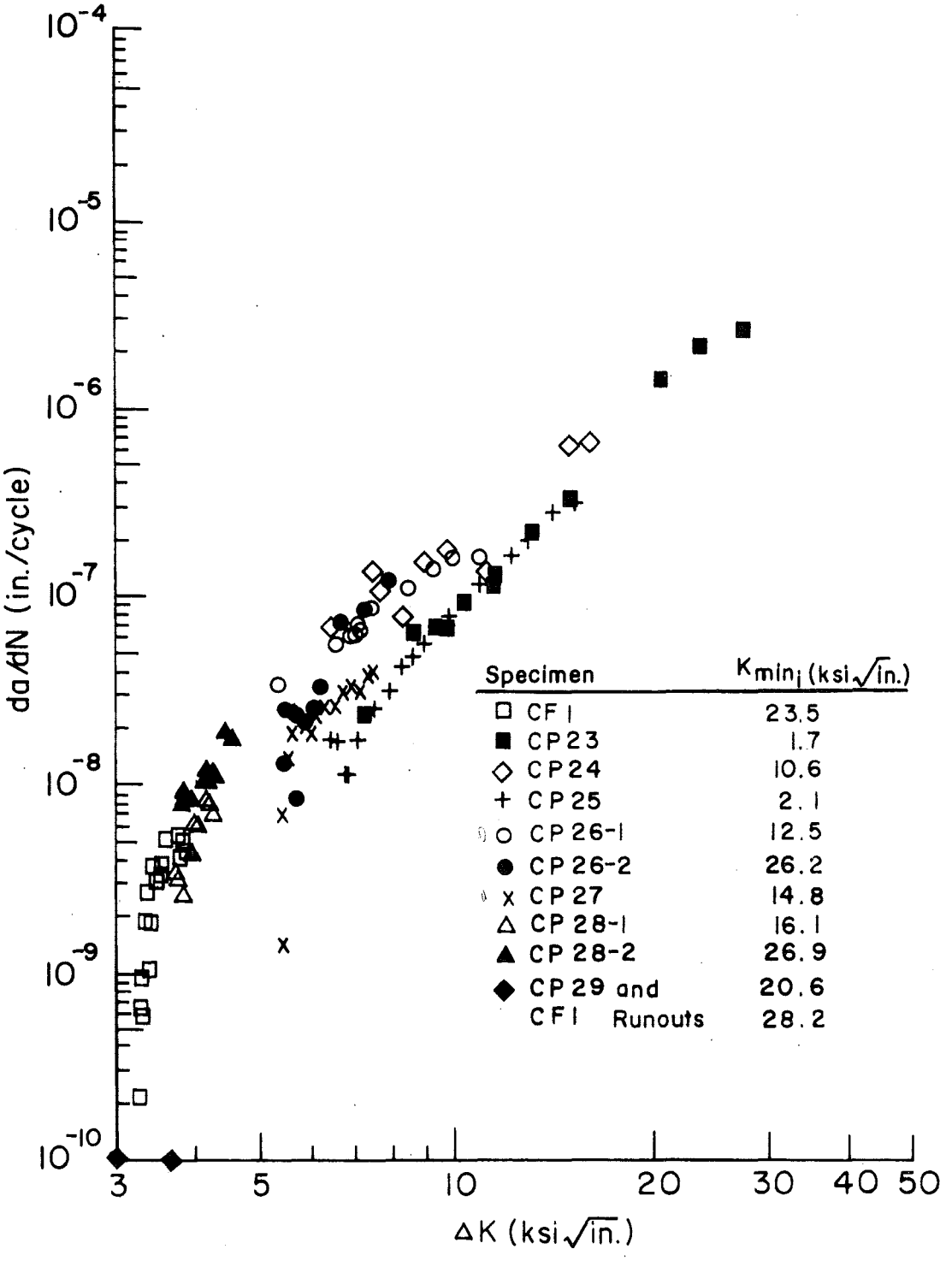

Fig. 15 Effect of the Minimum Stress Variable

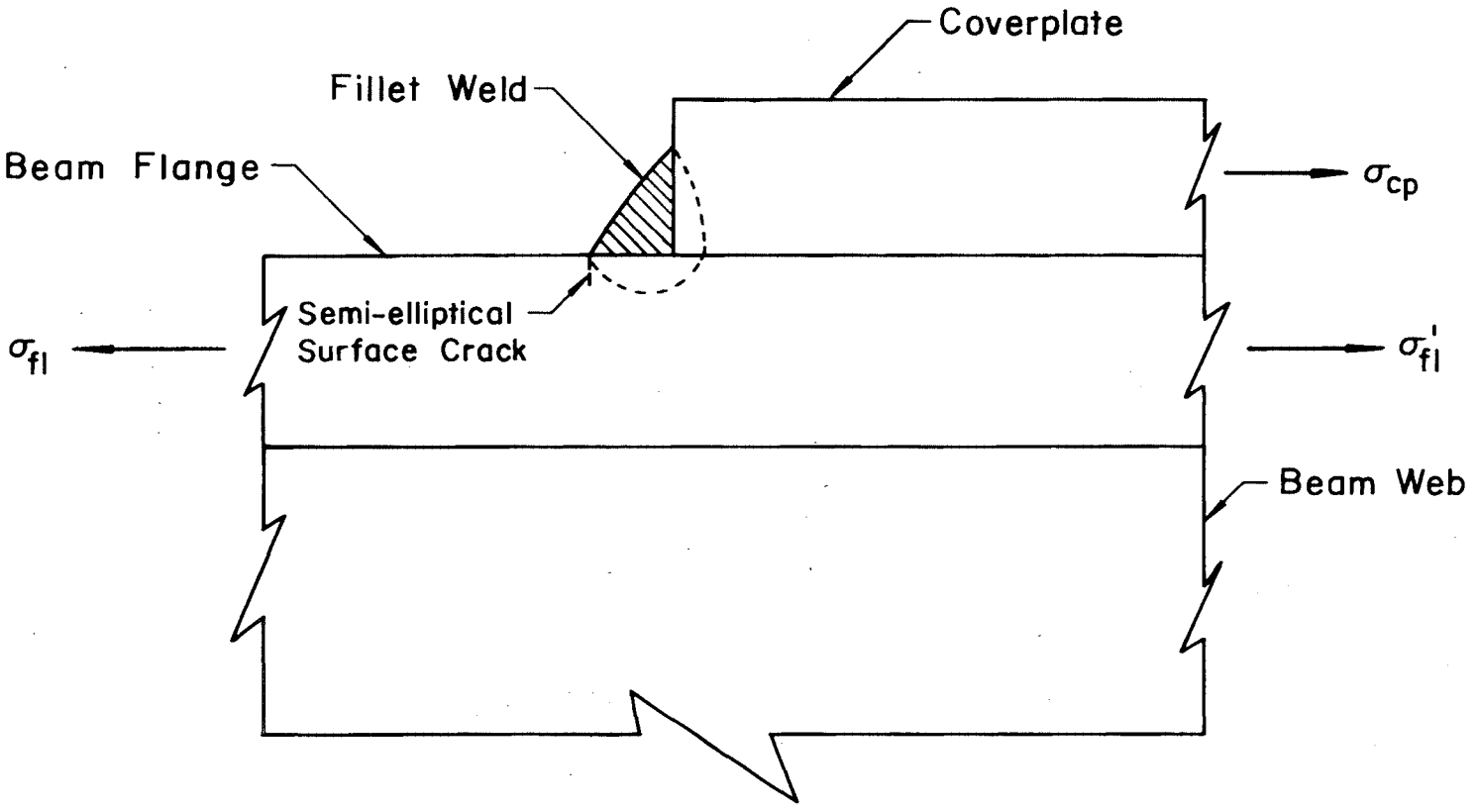

Fig. 16 Geometry of Cover Plate Welded to Beam Flange

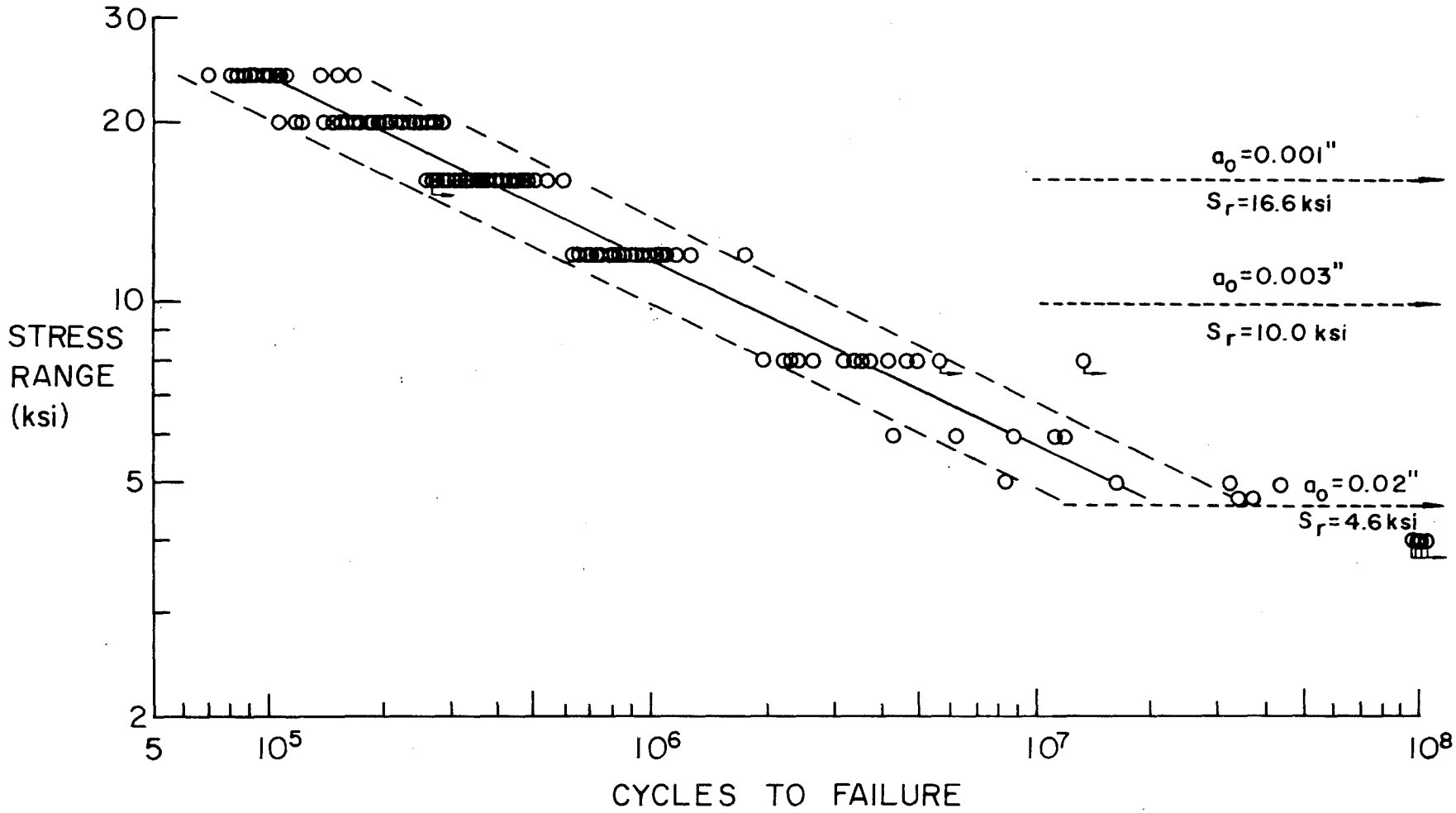

Fig. 17 Cover-Plated Beam Failures and Predicted Runout

REFERENCES

1. Fisher, J. W., Frank, K. H., Hirt, M. A. and McNamee, B. M.
   EFFECT OF WELDMENTS ON THE FATIGUE STRENGTH OF STEEL BEAMS, NCHRP Report No. 102, Highway Research Board, National Academy of Sciences-National Research Council, Washington, D.C., 1970.

2. Gurney, T. R.
   FATIGUE OF WELDED STRUCTURES, Cambridge Press, 1968.

3. American Association for State Highway Officials
   STANDARD SPECIFICATIONS FOR HIGHWAY BRIDGES, AASHO, Washington, D.C., 1969.

4. American Institute of Steel Construction
   MANUAL OF STEEL CONSTRUCTION, AISC, New York, 1970.

5. Fisher, J. W., Albrecht, P. A. Yen, B. T., Klingerman, D. J. and McNamee, B. M.
   EFFECT OF WELDMENTS ON THE FATIGUE STRENGTH OF STEEL BEAMS - TRANSVERSE STIFFENERS AND ATTACHMENTS, Fritz Engineering Laboratory Report No. 334.10, Lehigh University, Sept. 1972.

6. Frank, K. H.
   THE FATIGUE STRENGTH OF FILLET WELDED CONNECTIONS, Ph.D. Dissertation, Lehigh University, Oct. 1971.

7. Frank, K. H. and Fisher, J. W.
   ANALYSIS OF ERROR IN DETERMINING FATIGUE CRACK GROWTH RATES, Fritz Engineering Laboratory Report No. 358.10, Lehigh University, March 1971.

8. Irwin, G. R., Liebowitz, H. and Paris, P. C.
   A MYSTERY OF FRACTURE MECHANICS, Engineering Fracture Mechanics, Vol. 1 No. 1, June 1968.

9. Paris, P. C. and Sih, G. C.
   STRESS ANALYSIS OF CRACKS, Special Technical Publication 381, ASTM, 1970.

10. Paris, P. C. and Erdogan, F.
    A CRITICAL ANALYSIS OF CRACK PROPAGATION LAWS, Transactions, ASME, Journal of Basic Engineering, Vol. 85, Series D, No. 4, 1963.

11. Gurney, T. R.
    AN INVESTIGATION OF THE RATE OF PROPAGATION OF FATIGUE CRACKS IN A RANGE OF STEELS, The Welding Institute Research Report No. E18/12/68, Dec. 1968.

12. Barsom, J. M.
FATIGUE-CRACK PROPAGATION IN STEELS OF VARIOUS YIELD STRENGTHS, U. S. Steel Corp., Applied Research Laboratory, Monroeville, Pennsylvania, 1971.

13. Klingerman, D. J., Frank, K. H. and Fisher, J. W.
FATIGUE CRACK GROWTH IN A36 STEEL, Fritz Engineering Laboratory Report No. 358.31, Lehigh University, May 1971.

14. Hirt, M. A. and Fisher, J. W.
FATIGUE BEHAVIOR OF WELDED BEAMS, Highway Research Record No. 400, Highway Research Board, National Academy of Sciences-National Research Council, Washington, D. C., 1972.

15. Paris, P. C.
TESTING FOR VERY SLOW GROWTH OF FATIGUE CRACKS, Closed Loop, MTS Systems Corp., Vol. 2, No. 5, 1970.

16. Paris, P. C. and Wei, R. P.
FRACTURE MECHANICS IN FATIGUE, ASM Symposium on Engineering Aspects of Fatigue, Materials Engineering Congress, Philadelphia, Pa., Oct. 1969.

17. Johnson, R. E.
SOME OBSERVATIONS OF CYCLIC CRACK PROPAGATION FROM A FRACTURE MECHANICS VIEWPOINT, ASM Symposium of Metallurgical Aspects of Fatigue Fracture, Materials Engineering Congress, Philadelphia, Pa., Oct. 1969.

18. Harrison, J. D.
AN ANALYSIS OF DATA ON NON-PROPAGATION FATIGUE CRACKS ON A FRACTURE MECHANICS BASIS, Metal Construction and British Welding Journal, Vol. 2, No. 3, March 1970.

19. Irwin, G. R.
CRACK EXTENSION FORCE FOR A PART-THROUGH CRACK IN A PLATE, Transactions, ASME, Series E, Vol. 24, No. 3, Sept. 1957.

20. Albrecht, P. A.
FATIGUE STRENGTH OF WELDED BEAMS WITH STIFFENERS, Ph.D. Dissertation, Lehigh University, July 1972.

21. Signes, E. G., Baker, R. G., Harrison, J. D. and Burdekin, F. M.
FACTORS AFFECTING THE FATIGUE STRENGTH OF WELDED HIGH STRENGTH STEELS, British Welding Journal, Vol. 14, March 1967.